Chem. Eur. J. **2000**.

Sequence-dependent Bending of DNA induced by Cisplatin: NMR Structures of an A·T Rich 14-mer Duplex

John A. Parkinson, Yu Chen, Zijian Guo, Piedad del Socorro Murdoch, Susan J. Berners-Price, Tom Brown and Peter J. Sadler

Supporting Information

Table S1: ^{1}H chemical shift assignments (ppm) for the platinated duplex **III***: d(ATACATG*G*TACATA)•(TATGTACCATGTAT).

Base	H8	H6	H2	H5	CH_3	H1'	H2'	H2"	H3'	H4'	H5'/H5"	GH1/TH3	H42	H41
A1	8.20		7.94			6.21	2.69	2.85	4.87	4.27	3.81			
T2		7.41			1.37	5.61	2.20	2.48	4.91	4.23	4.12			
A3	8.31		7.54			6.24	2.73	2.90	5.06	4.46	-[a]			
C4		7.36		5.29		5.50	2.12	2.39	4.84	4.23	-		8.12	6.59
A5	8.25		7.58			6.18	2.63	2.83	-	-	-			
T6		7.14			1.41	5.86	1.37	2.37	4.79	4.29	4.11/4.06	13.96		
G7	8.64					6.08	2.50	2.72	5.09	4.23	4.15/4.07	13.50		
G8	8.08					5.58	2.23	2.55	4.64	4.18	4.08	13.06		
T9		7.48			1.31	5.83	2.27	2.63	4.91	4.24	-	13.80		
A10	8.28					6.21	2.67	2.90	5.03	4.41	-			
C11		7.32		5.30		5.51	2.05	2.37	4.84	4.19	-		8.17	6.63
A12	8.28		7.63			6.18	2.59	2.84	-	-	-			
T13		7.18			1.48	5.80	1.90	2.27	4.81	4.11	4.11/4.08			
A14	8.22		7.47			6.28	2.67	2.43	4.70	4.20	-			
T15		7.37			1.56	5.78	1.85	2.25	4.68	4.02	3.65			
A16	8.50		7.80			6.37	2.88	3.05	5.05	4.47	4.14/4.05			
T17		7.27			1.42	5.77	2.22	2.50	4.90	4.27	-	13.39		
G18	7.85					5.99	2.63	2.78	4.94	4.41	4.23/4.19	12.46		
T19		7.32			1.42	5.81	2.22	2.56	4.91	-	-	13.53		
A20	8.29					6.21	2.62	2.83	-	4.38	-			
C21		7.40		5.46		5.88	1.97	2.36	4.73	4.09	4.28		8.39	6.92
C22		7.47		5.47		5.52	2.02	2.36	4.79	4.06	3.93		7.87	6.80
A23	8.34		7.81			6.24	2.77	2.93	5.02	4.37	-			
T24		7.20			1.38	5.73	2.17	2.45	4.89	4.21	-	13.36		
G25	7.85					5.94	2.61	2.76	4.95	4.39	4.21/4.14	12.42		
T26		7.25			1.45	5.74	2.06	2.45	4.88	4.21	-	13.55		
A27	8.31		7.56			6.29	2.74	2.90	-	4.42	-			
T28		7.25			1.48	6.09	2.14	2.14	4.52	4.02	4.31/4.08			

-[a] resonances unassigned

Table S2: ^{1}H chemical shift assignments (ppm) for the unmodified duplex **III**: d(ATACATGGTACATA)•(TATGTACCATGTAT).

Base	H8	H6	H2	H5	CH_3	H1'	H2'	H2"	H3'	H4'	H5'/H5"	GH1/TH3	H42	H41
A1	8.16		7.66			6.20	2.65	2.80	4.86	4.26	3.79			
T2		7.37			1.46	5.65	2.16	2.43	4.87	4.23	4.20/4.12			
A3	8.30		7.59			6.24	2.72	2.90	5.04	4.44	4.11/4.20			
C4		7.31		5.31		5.56	2.05	2.40	4.81	4.22	4.22/4.16		8.09	6.52
A5	8.20		7.50			6.19	2.60	2.88	4.98	4.39	4.17/4.11			
T6		7.04			1.35	5.71	1.92	2.35	4.84	4.29	4.22/4.13	13.54		
G7	7.75					5.66	2.63	2.66	4.95	4.23	-[a]/4.04	12.55		
G8	7.56					5.89	2.46	2.69	4.85	4.37	-/4.18	12.69		
T9		7.19			1.33	5.71	2.05	2.46	4.85	4.24	4.12/4.17	13.48		
A10	8.23		7.38			6.17	2.66	2.85	5.00	4.41	4.10/4.17			
C11		7.27		5.30		5.51	1.97	2.33	4.81	4.16	-/4.15		8.13	6.52
A12	8.21		7.66			6.18	2.56	2.80	4.97	4.35	4.16/4.10			
T13		7.14			1.49	5.86	1.90	2.25	4.80	4.11	4.16/4.08			
A14	8.21		7.47			6.28	2.65	2.46	4.70	4.18	4.16/4.09			
T15		7.31			1.55	5.81	1.78	2.20	4.64	4.00	3.64			
A16	8.44		7.84			6.34	2.87	3.00	5.02	4.45	4.12/4.05			
T17		7.22			1.43	5.77	2.16	2.48	4.87	4.27	4.18/4.25	13.40		
G18	7.82					5.96	2.57	2.74	4.93	4.37	4.25/4.17	12.42		
T19		7.22			1.41	5.71	2.07	2.45	4.87	-	4.13/4.17	13.48		
A20	8.23		7.37			6.17	2.66	2.86	5.00	4.40	4.10/4.17			
C21		7.24		5.22		5.77	1.98	2.39	4.72	4.30	4.09/4.05		7.96	6.40
C22		7.42		5.48		5.50	2.07	2.40	4.82	4.10	4.09/4.05		8.33	6.62
A23	8.27		7.59			6.22	2.65	2.92	5.00	4.41	4.16/4.06			
T24		7.09			1.42	5.72	2.05	2.40	4.85	4.21	4.25/4.16	13.51		
G25	7.76					5.89	2.54	2.69	4.91	4.35	4.16/4.13	12.37		
T26		7.17			1.41	5.78	1.97	2.38	4.85	4.21	4.12/4.17	13.40		
A27	8.26		7.61			6.29	2.73	2.84	5.00	4.40	4.14/4.17			
T28		7.29			1.55	6.10	2.16	2.16	4.52	4.04	4.26/4.09			

-[a] resonance unassigned

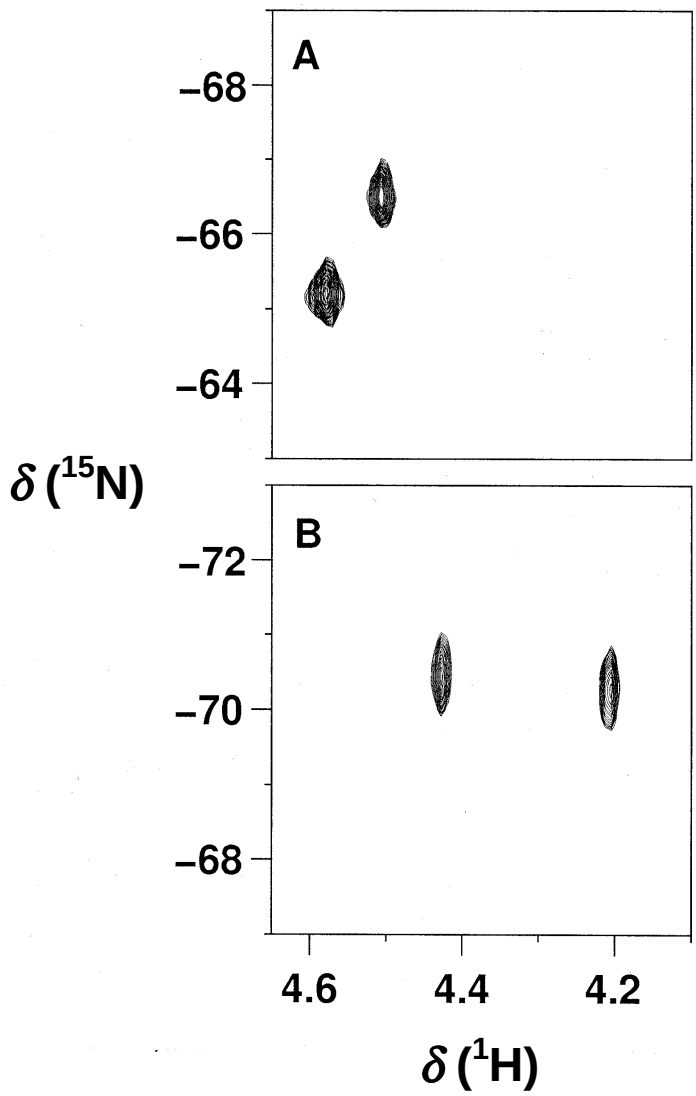

Figure S1: **2D [^{1}H, ^{15}N] HSQC NMR data for I* and III*.** 2D [^{1}H, ^{15}N] HSQC NMR spectra (acquired at 298 K) for (A) the HPLC purified platinated G*G* 14-mer DNA single strand, **I***, and (B) the platinated 14-mer DNA duplex, **III***, formed by annealing **I*** with its complementary CC strand (0.1 M $NaClO_4$, pH 6.0, 9 mM phosphate buffer, 90% H_2O/10% D_2O). Only one pair of cross-peaks is observed in each spectrum which suggests that there is predominantly a single conformation for the $\{Pt(NH_3)_2\}^{2+}$ adducts of the single strand and the duplex. Peak assignments were made according to previous work.[18]

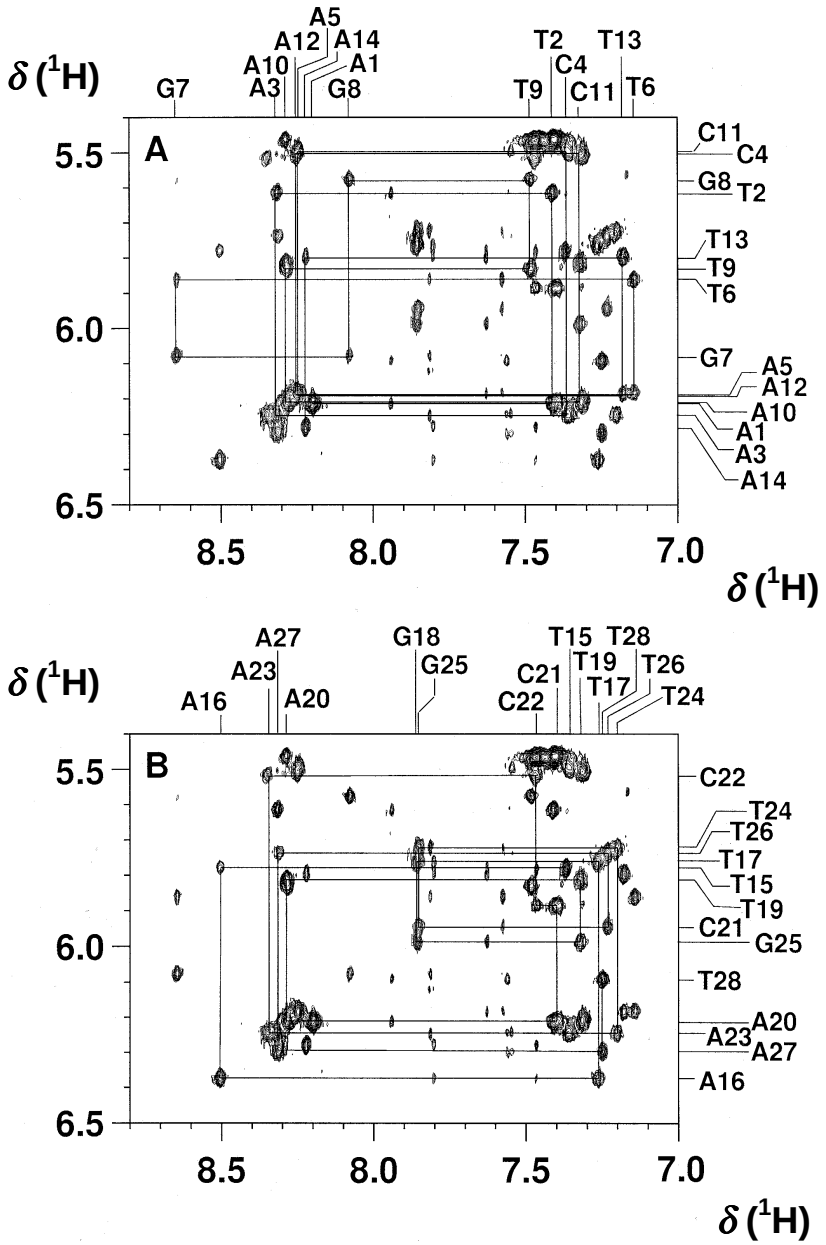

Figure S2: ^{1}H NMR data assignment of III*. Duplicate contour plots of the 2D NOESY NMR spectrum (300 ms mixing time, 99.9% D_2O, 278 K) of **III*** showing the aromatic (8.7-7.0 ppm) to sugar ring H1' (6.5-5.4 ppm) connectivities. The sequential NOESY assignment walks are shown (A) for the platinated G*G* strand and (B) for the complementary CC strand of the duplex **III***.

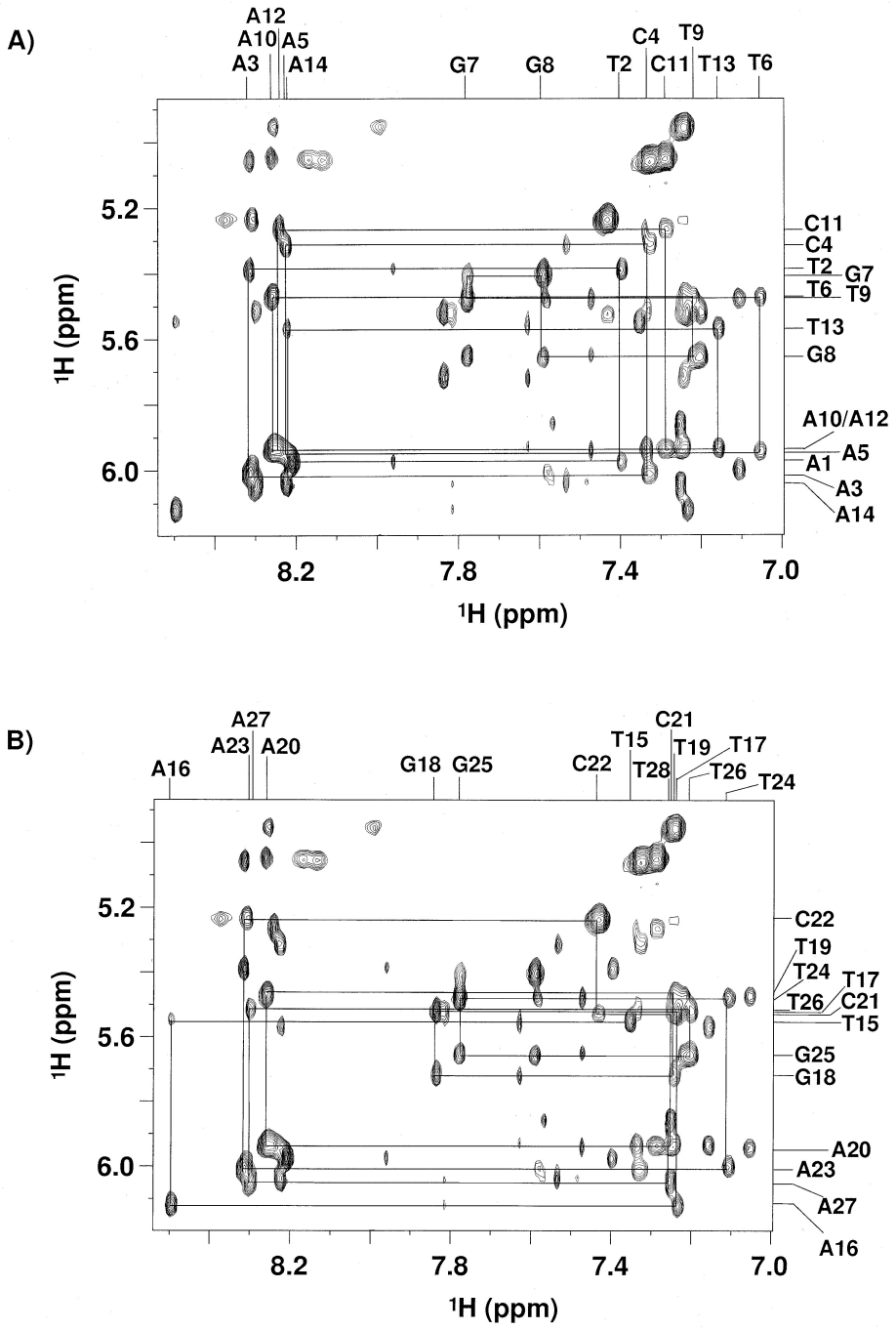

Figure S3: ^{1}H NMR data assignment for III. Duplicate contour plots of the 2D NOESY NMR spectrum of the unplatinated DNA duplex **III** (300 ms mixing time, 99.9% D_2O) showing the aromatic to H1' connectivities. The sequential NOESY assignment walks are shown in (A) for the GG strand, and (B) for the complementary CC strand.

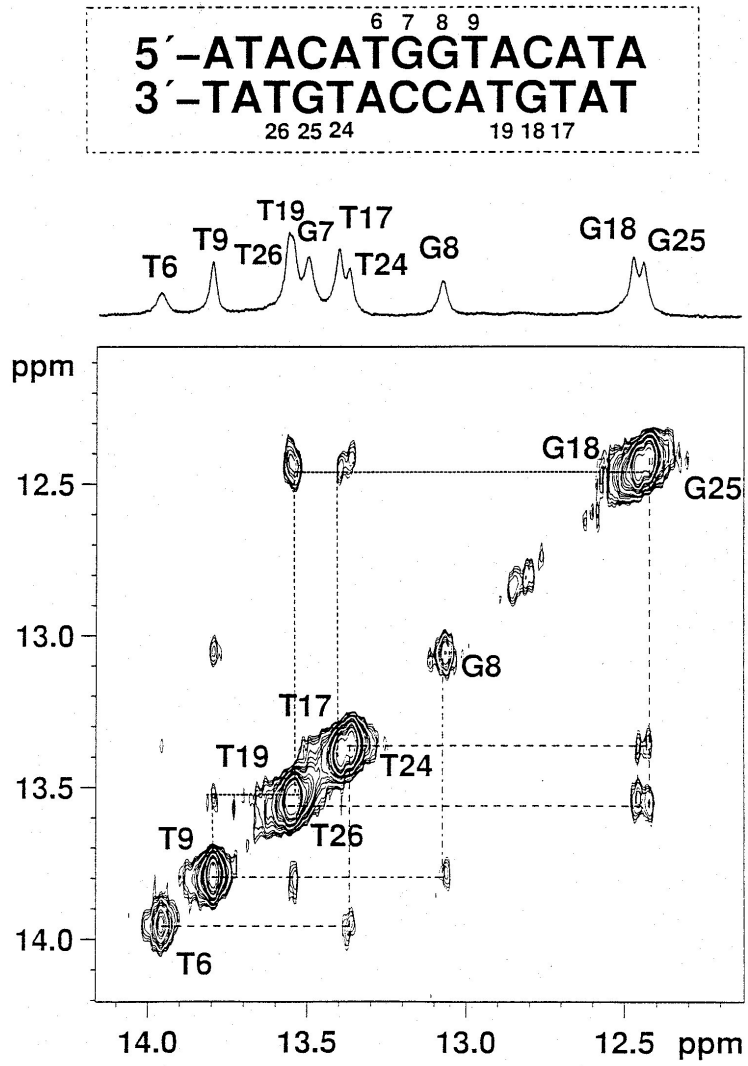

Figure S4: Assignment of imino proton resonances of III*. Contour plot of the 150 ms 2D NOESY NMR spectrum of **III*** at 278 K in 90% H_2O/10% D_2O showing the imino-to-imino cross-peak region. The sequential assignment connectivities between the imino protons involved in Watson-Crick hydrogen bonding are shown, with an interruption only at the G7* site. The imino proton resonances from the two base-pairs at either ends of the duplex (A1/T28, T2/A27; T13/A16, A14/T15) are not observed. The 1D ^1H NMR spectrum of the same region is shown at the top of the figure.

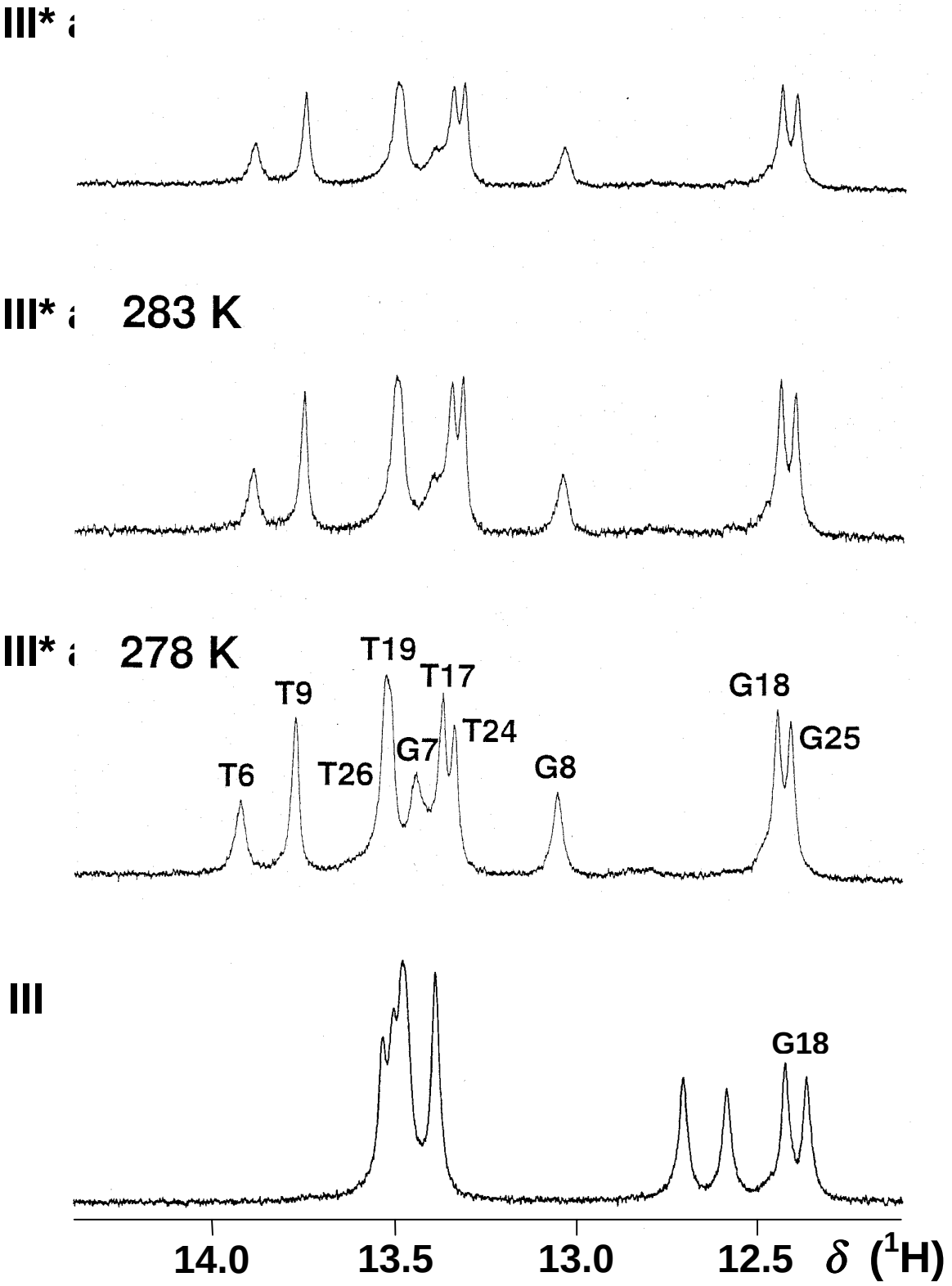

Figure S5: The imino region of the 1D ^{1}H NMR spectra of III* and III. Variable temperature data for **III*** showing the appearance of the G7* imino proton at low temperature. The same region of the 1D ^{1}H NMR spectrum of **III** at 278 K is also shown with signal assignments for comparison (bottom spectrum).

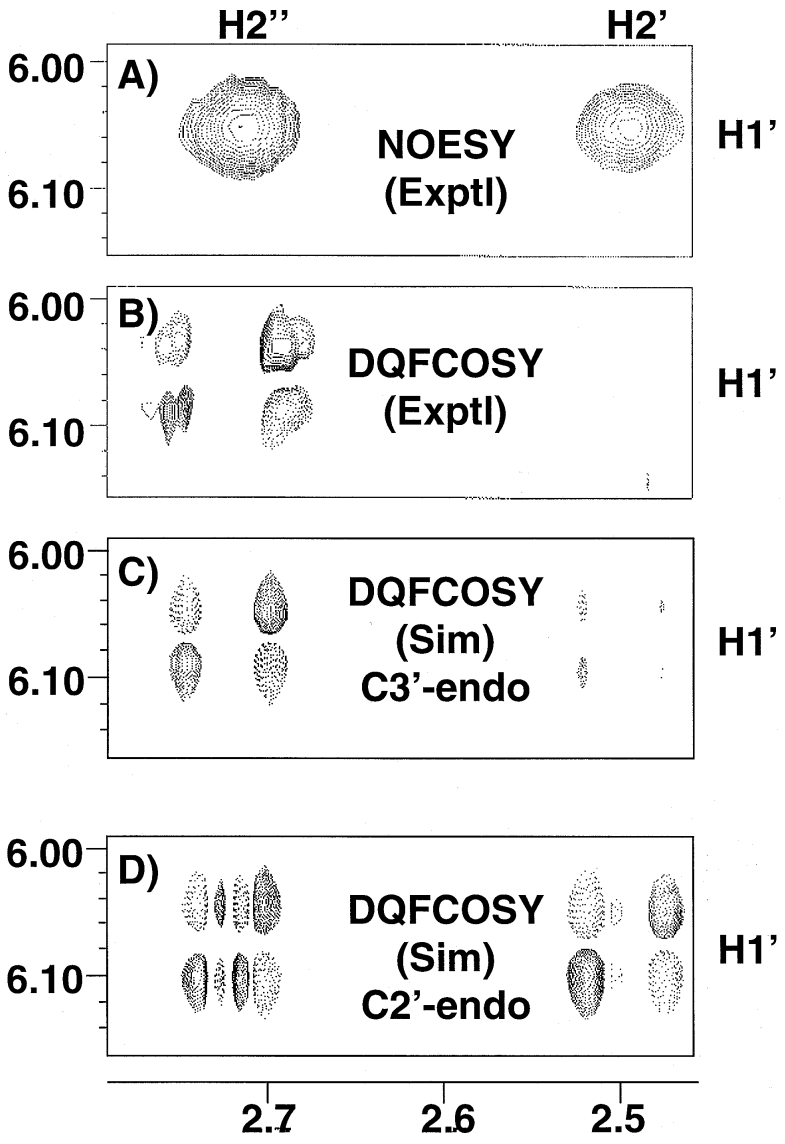

Figure S6: H1'-H2' and H1'-H2'' cross-peaks for the G7* residue of III*. A) Experimental NOESY data; B) experimental DQFCOSY data; C) DQFCOSY cross-peak simulation using the programs SPHINX and LINSHA for a C3'-endo sugar ring conformation; D) as for C but for a sugar ring in the C2'-endo conformation. The similarity between B and C reveals that the sugar ring of G7* adopts a C3'-endo conformation. Pairs of cross-peaks for the remaining sugar rings were similar to those in D in the experimental DQFCOSY data.

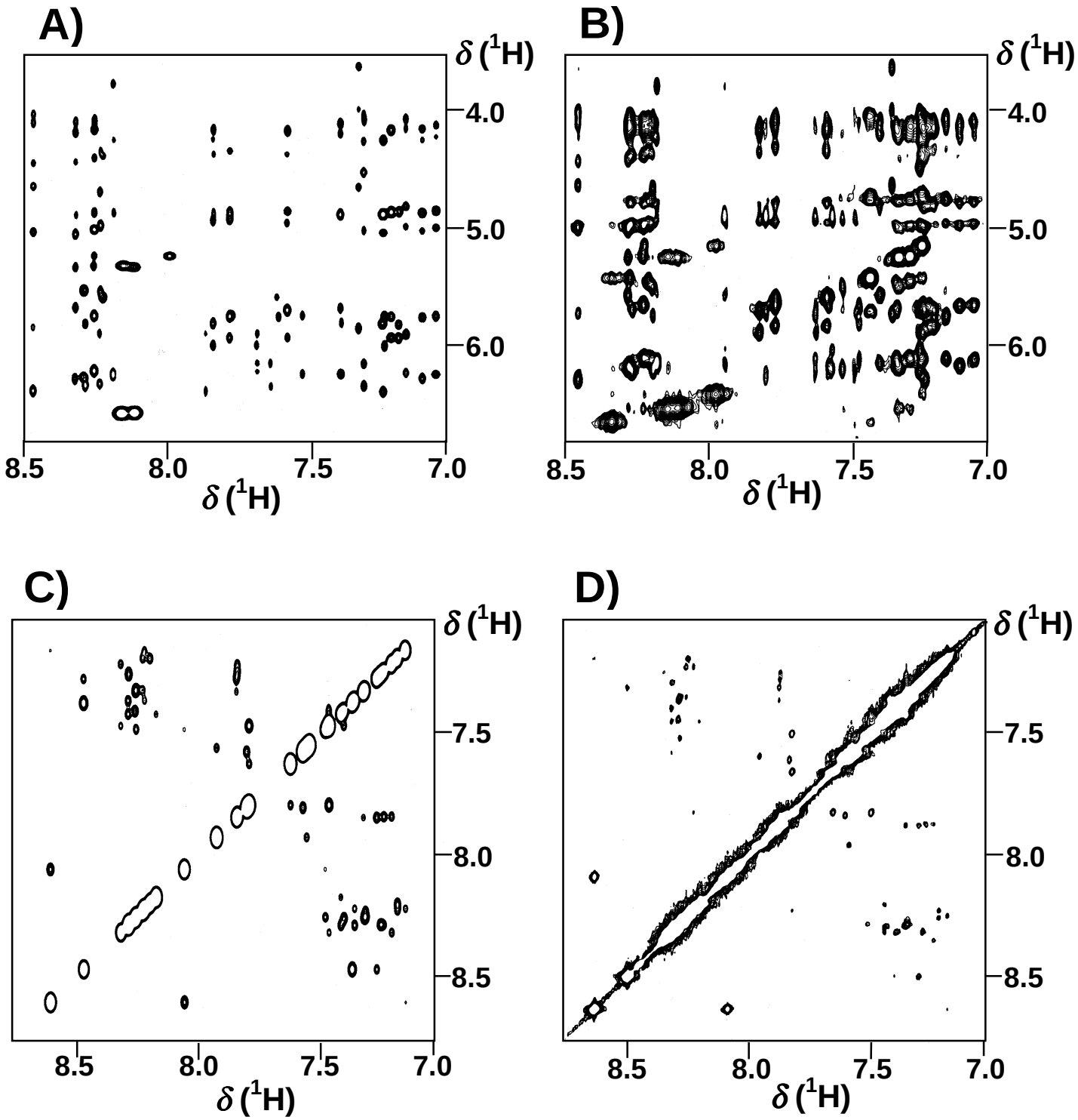

Figure S7: Comparison of calculated vs experimental nOe data for III and III*. Calculated **(A)** and experimental **(B)** data covering the aromatic to sugar H1'/H3'/H4'/H5'/H5" nOe correlation region are shown for **III**. Calculated **(C)** and experimental **(D)** data in the aromatic region of the nOe data are shown for **III***.

A)

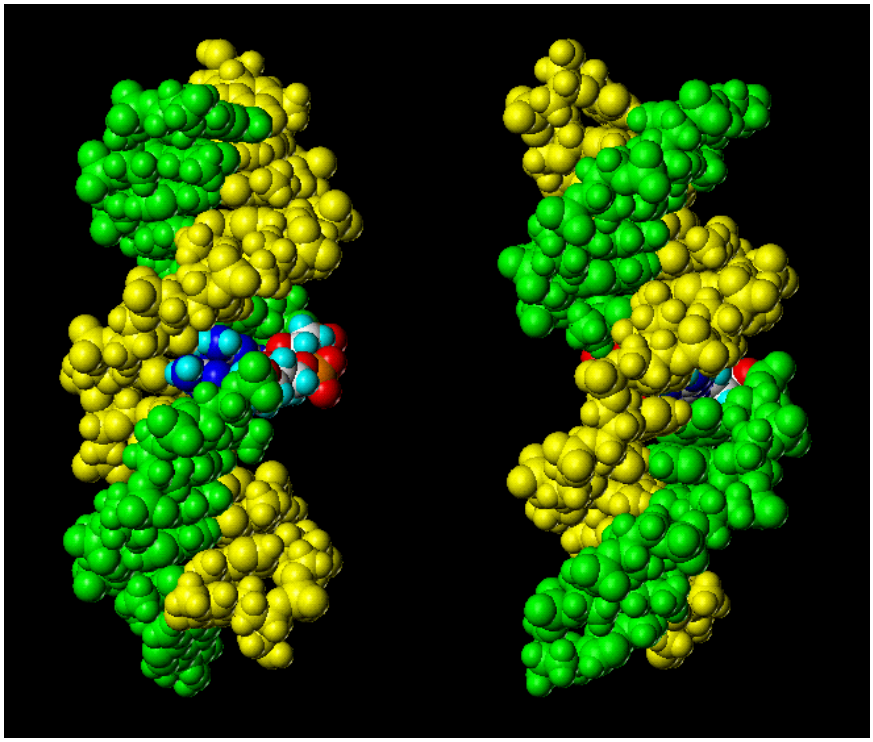

B)

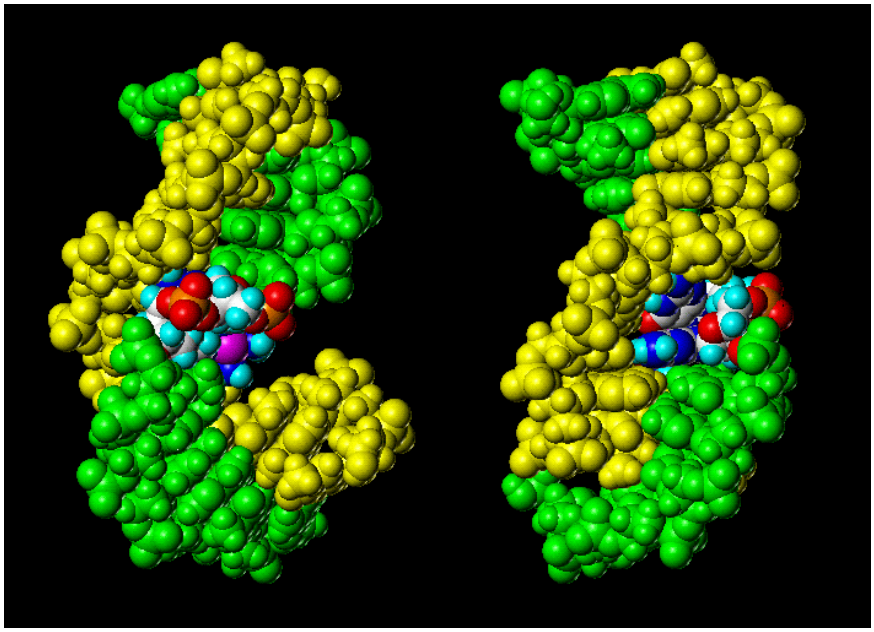

Figure S8: Space-filling models of III and III*. Orthographic representations of A) **III**, and B) **III***, calculated from NMR data. Colour coding: GG strand - green; complementary CC strand - yellow; central GG residues coloured by atom type; platinum atom - magenta.

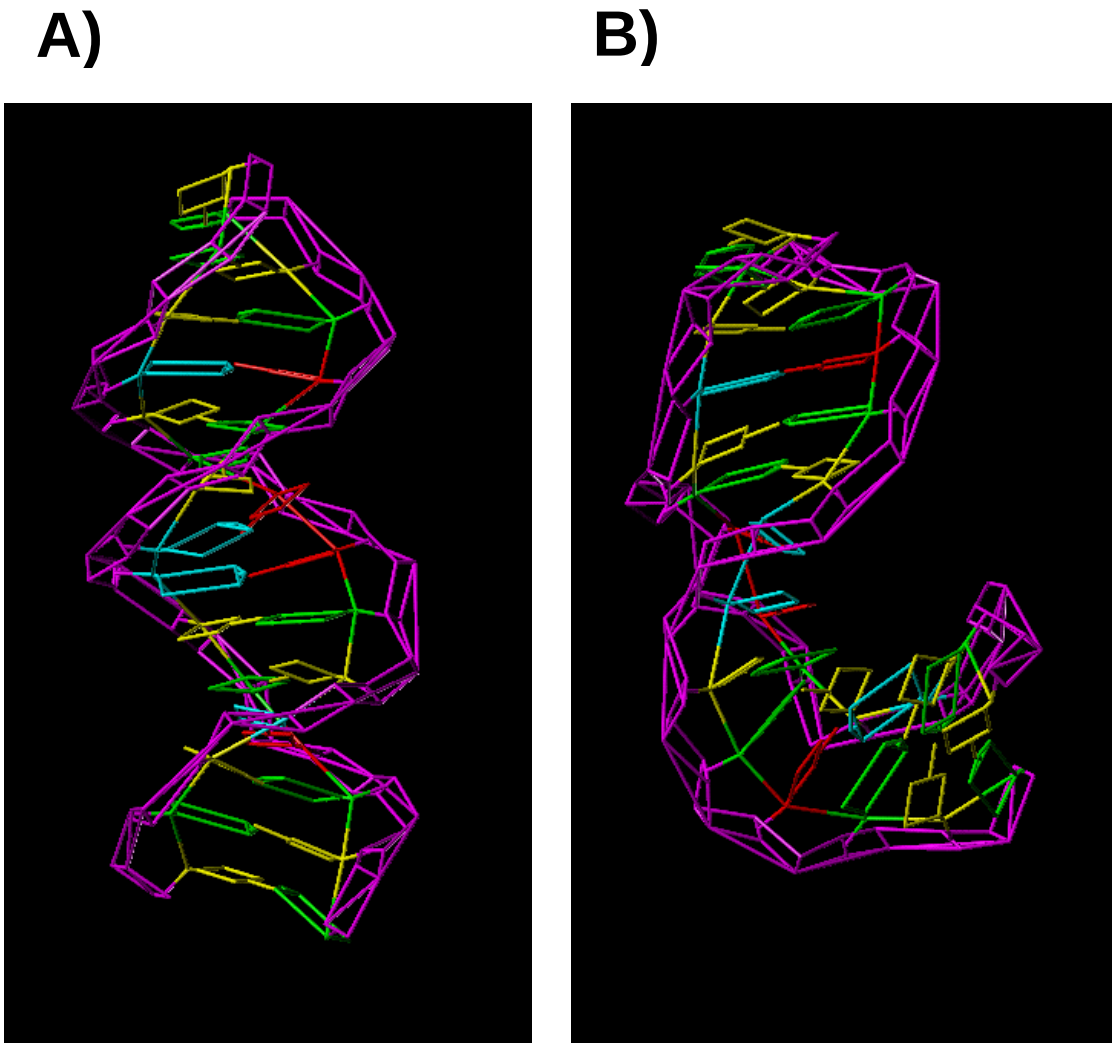

Figure S9: Cartoon representations of III and III*. Line models of A) **III**, and B) **III***, calculated using the program CURVES. Models are the average of a family of 10 structures. Bases are colour coded: A - green; T - yellow; G - blue; C - red.

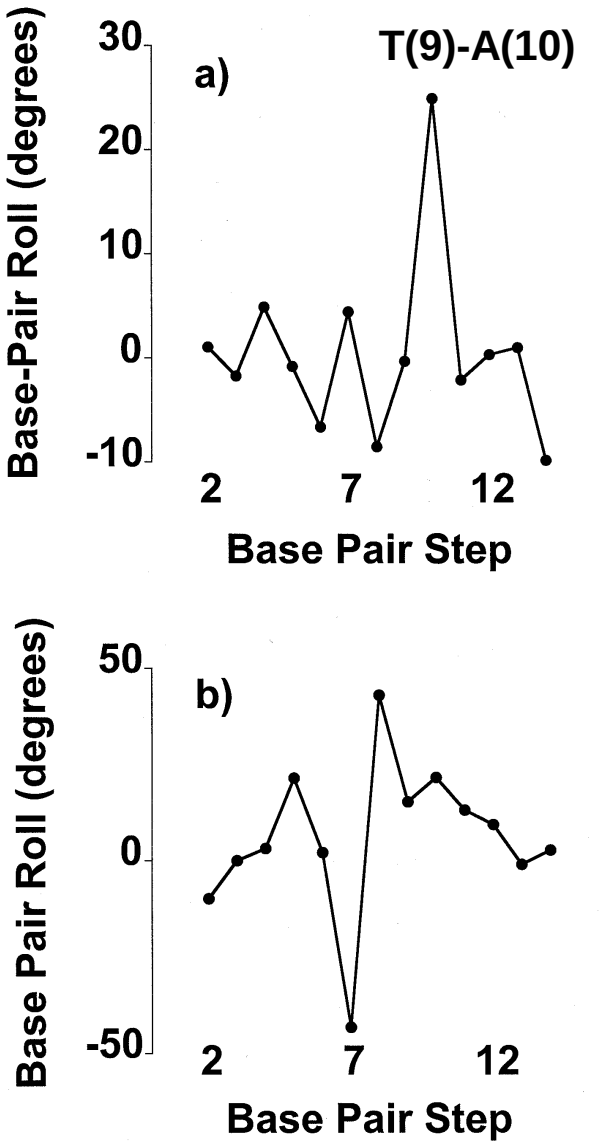

Figure S10: Variation in inter base-pair roll (°) with base-pair step. Inter base-pair roll a) for **III**; b) for **III*** calculated using the program CURVES from an average model for each structure. The largest inter base-pair roll for **III** occurs at the T9-A10 step. The largest inter base-pair roll for **III*** occurs at the G7-G8 step.